Table 6. *Interatomic distances* (Å) *in* $Cs_2CaCl_4.2H_2O$

Cs—Cl(1)	3·447 (3) Å	O—Cl(1)	3·153 (9) Å
—Cl(1)	3·492 (3)	—Cl(2)	3·267 (12)
—Cl(2)	3·536 (3)	—Cl(2)	3·549 (9)
—Cl(2)	3·545 (3)	—Cl(1)	3·613 (10)
—Cl(1)	3·571 (3)	—Cl(1)	3·626 (13)
—Cl(1)	3·604 (3)	—Cl(2)	3·649 (13)
—Cl(2)	3·710 (4)	—Cl(2)	3·786 (9)
—Cl(1)	3·831 (4)	—Cl(1)	3·888 (13)
—O	3·624 (9)		
—O	3·833 (11)	Ca—Cl(2)(×2)	2·711 (3)
—O	4·151 (12)	—Cl(1)(×2)	2·739 (3)
—O	4·165 (9)	—O(×2)	2·367 (12)

face centers between pairs of H_2O molecules. Ca atoms are coordinated octahedrally as $CaCl_4(H_2O)_2$. Chain formation is not required for charge balance in this structure, and the H_2O–Ca–H_2O groups are isolated from each other. The cubic chlorine framework is only a little more distorted than in the Na compound. Hydrogen bonds are formed between H_2O molecules and the pair of Cl atoms at one cube edge opposite the Ca atom, as in the Na compound. Table 6 lists the bond lengths in the structure.

A subsequent search for other double-salt hydrates containing CsCl that might follow a structural principle similar to that found in this work led to two other compounds: $Cs_2MnCl_4.2H_2O$ and $Rb_2MnCl_4.2H_2O$. The structures of these crystals have been reported by Jensen (1964). They are, in fact, isostructural with $Cs_2CaCl_4.2H_2O$. After transforming Jensen's unit cells by $(00\bar{1}/100/0\bar{1}0)$, they may be compared with that given in the *Abstract* as follows:

	$Cs_2CaCl_4.2H_2O$	$Cs_2MnCl_4.2H_2O$	$Rb_2MnCl_4.2H_2O$
a (Å)	6·904	6·66	6·48
b (Å)	7·513	7·27	7·01
c (Å)	5·877	5·74	5·66
α (°)	92·28	92·2	92·3
β (°)	96·13	95·7	95·2
γ (°)	65·23	67·0	66·7
V (Å^3)	275·2	254·6	232·3.

References

CHOU, I.-M. & LEE, R. D. (1983). *J. Chem. Eng. Data*, **28**, 390–393.

CHOU, I.-M. & ROMANKIW, L. A. (1983). *J. Chem. Eng. Data*, **28**, 396–398.

CHOU, I.-M., ROMANKIW, L. A., EVANS, H. T. JR & KONNERT, J. A. (1982). *Trans. Geophys. Union*, **63**, 465.

CHOU, I.-M., ROMANKIW, L. A., EVANS, H. T. JR & KONNERT, J. A. (1983). *J. Chem. Eng. Data*, **28**, 393–396.

CROMER, D. T. & MANN, J. B. (1968). *Acta Cryst.* A**24**, 321–324.

EVANS, H. T. JR, KONNERT, L. A., CHOU, I.-M. & ROMANKIW, L. A. (1982). *Am. Crystallogr. Assoc. Progr. Abstr.* **10**, 32.

JAMIESON, G. S. (1917). *Am. J. Sci.* **43**, 67–68.

JENSEN, S. J. (1964). *Acta Chem. Scand.* **18**, 2085–2097.

PLYUSHCHEV, V. E., TULINOVA, V. B., KUTZNETSOVA, G. P., KOROVIN, S. S. & PETROVA, R. G. (1957). *Zh. Neorg. Khim.* **2**, 2212–2220; Engl. trans. *J. Inorg. Chem. USSR*, **2**, 357–368.

PLYUSHCHEV, V. E., TULINOVA, V. B., KUTZNETSOVA, G. P., KOROVIN, S. S. & SHIPETINA, N. S. (1957). *Zh. Neorg. Khim.* **2**, 2654–2660; Engl. trans. *J. Inorg. Chem. USSR*, **2**, 267–275.

PÖYHÖNEN, J. & RUUSKANEN, A. (1964). *Ann. Acad. Sci. Fenn. Ser. A*, **6**, No. 146, 1–12.

STEWART, J. M. (1976). Editor, XRAY76. Tech. Rep. TR-446, Computer Science Center, Univ. of Maryland, College Park, Maryland.

SWANSON, H. E. & FUYAT, R. K. (1953). *Natl Bur. Stand. US Circ.* 539, Vol. II, 41–43.

ZEMCZUZNY, S. & RAMBACH, F. (1910). *Z. anorg. Chem.* **65**, 403–428.

Acta Cryst. (1984). B**40**, 92–96

Electron Density Distribution in an Ilmenite-Type Crystal of Cobalt(II) Titanium(IV) Trioxide

BY KUMIKO KIDOH, KIYOAKI TANAKA AND FUMIYUKI MARUMO

The Research Laboratory of Engineering Materials, Tokyo Institute of Technology, Nagatsuta 4259, *Midori-ku, Yokohama* 227, *Japan*

AND HUMIHIKO TAKEI

Research Institute for Iron, Steel and Other Metals, Tohoku University, Sendai 980, *Japan*

(*Received* 23 *July* 1983; *accepted* 25 *October* 1983)

Abstract

The electron density distribution in a crystal of $CoTiO_3$ has been investigated with the single-crystal X-ray diffraction method. Deformation densities were observed around the Co^{2+} ion, which is qualitatively explained with the high-spin electron configuration of a d^7 ion in an octahedral field. The Ti^{4+} ion lies in a negative region of the deformation density map, and a positive peak exists on the threefold axis at a position 0·63 Å from the Ti^{4+} ion towards the Co^{2+} ion. It is proposed that these negative and positive peaks are caused by deformation of the electron cloud to shield the positive charge of the neighbouring Co^{2+}

0108-7681/84/020092-05$01.50

ion. A small amount of partial disorder was observed in the cation arrangement of the crystal examined. [Crystal data: $R\bar{3}$, $a = 5{\cdot}0662\,(2)$, $c = 13{\cdot}918\,(1)$ Å, $Z = 6$, $D_x = 4{\cdot}998$ g cm^{-3}, $\mu(\mathrm{Mo}K\alpha) = 115{\cdot}5$ cm^{-1}.]

Introduction

Recently, Vincent, Yvon, Grüttner & Ashkenazi (1980) and Vincent, Yvon & Ashkenazi (1980) reported the results of investigations on electron density distributions in crystals of Ti_2O_3 and V_2O_3; these represent the two extremes of the c/a ratio for corundum-type sesquioxides. They observed deformation densities of d electrons suggesting metal–metal interactions around the metal atoms and metal–O bond formation around the O atoms. The distributions of the deformation densities around the metal atoms are quite different in each of these crystals. Vincent *et al.* interpreted the difference by assuming that the metal–metal interaction occurs mainly *via* σ bonds across the common faces of the coordination octahedra in Ti_2O_3, whereas the interaction occurs *via* π bonds across the common edges in V_2O_3.

Ilmenite, $FeTiO_3$, has the same structure as that of corundum but it contains two kinds of metal atoms with an ordered arrangement. Since a variety of ilmenite-type crystals are known, it is of interest to examine the relation between the structural features and electron density distributions in these crystals. In this study, the electron density distribution in a crystal of $CoTiO_3$ was investigated with the X-ray diffraction method as part of a systematic study on ilmenite-type crystals of the first-series transition-metal elements.

Experimental

A crystal synthesized with an infrared-heating floating-zone furnace (Takei, Hosoya & Kojima, 1982) was used in this study. A piece of the crystal was shaped into a sphere 0·16 mm in diameter by the Bond (1951) method in order to ensure constant illumination of X-rays on the specimen and to facilitate the intensity corrections. Weissenberg photographs confirmed that the crystal had an ilmenite-type structure. After these procedures, the specimen was mounted on a Rigaku automated four-circle diffractometer (AFC-5).

The lattice constants were determined from 26 2θ values higher than 72° measured on the four-circle diffractometer with graphite-monochromated Mo $K\alpha_1$ radiation. The crystal data are given in the *Abstract*. Intensity data were collected in a quadrant of reciprocal space lower than 130° in 2θ. A total of 90 strong reflections were measured in the full reciprocal space in view of the corrections for anisotropic-extinction effects. Each reflection was repeatedly measured up to ten times to reduce the statistical counting error. Additional experimental conditions are summarized in Table 1. Corrections for Lp factors were carried out with the usual procedure. The absorption effect was corrected with the values of the absorption correction factors A^* tabulated in *International Tables for X-ray Crystallography* (1967). The mean path length $T = (\mathrm{d}A^*/\mathrm{d}\mu)/A^*$ was calculated for each reflection, where μ is the linear absorption coefficient and $\mathrm{d}A^*/\mathrm{d}\mu$ was obtained by numerical differentiation. The value T is required for the extinction correction. Weak reflections with $|F| < 4\sigma(|F|)$ were omitted from the data set.

Table 1. *Additional experimental conditions*

Scan technique	ω–2θ
Scan speed	2° min^{-1} in 2θ
Number of measured reflections	2283
Number of reflections used	1714
Independent reflections	1053

Refinement

Two kinds of least-squares refinements were carried out. One is the usual refinement with spherical scattering factors, and the other is the subsequent refinement employing the aspherical scattering factors for $3d$ electrons of the Co^{2+} ion (hereafter abbreviated as ASF refinement).

(*a*) *Refinement with spherical scattering factors*

For the starting model, the ideal ilmenite structure was assumed. Atomic scattering factors for Co^{2+} and Ti^{4+} ions and dispersion correction factors were taken from *International Tables for X-ray Crystallography* (1974). The scattering factor given by Tokonami (1965) was used for the O^{2-} ion. The refinement was carried out with a modified version of the full-matrix least-squares program *LINEX* including the extinction corrections after Becker & Coppens (1974*a*, *b*, 1975). The least-squares calculations assuming an anisotropic type II extinction effect with a Gaussian mosaic-spread distribution gave R and R_w values of 0·0138 and 0·0160, respectively, while those assuming an anisotropic type I extinction effect diverged. After this refinement the equivalent reflections were averaged to calculate difference Fourier maps. On the difference Fourier maps, there was a negative peak at the Co^{2+} site with a depth of $-1{\cdot}5$ e Å^{-3} and a positive peak at the Ti^{4+} site with a height of 1·1 e Å^{-3}. A difference Fourier map calculated with scattering factors for neutral atoms also yielded negative and positive peaks around Co^{2+} and Ti^{4+} ions, respectively. Refinement was continued on the assumption of the chemical formula $(Co_qTi_r)(Ti_uCo_v)O_{q+v+2(r+u)}$ by changing q,r, u and v with a normalization of the larger values between $q+r$ and $u+v$ to unity. The R and R_w values reduced to 0·0130 and 0·0133, giving

the values 0·95 (1), 0·04 (2), 0·95 (2) and 0·05 (1) for q, r, u and v, respectively. Therefore, the composition of the present crystal can be assessed as $(Co_{0\cdot95}Ti_{0\cdot05})(Ti_{0\cdot95}Co_{0\cdot05})O_3$ within the experimental errors.

(*b*) *ASF refinement*

The ASF refinement was carried out at first by assuming a D_{3d} crystal field for the octahedral cations. The aspherical scattering factors were employed only for the Co^{2+} ion at the octahedral site occupied mainly by Co^{2+}. When the octahedral crystal field is trigonally deformed, the t_{2g} orbitals split into a_g and e_g levels. The wavefunctions and the scattering factors for the respective orbitals are expressed in the following forms, by choosing the quantization axis z along the threefold axis and x in the plane determined by z and one of the Co–O bonds, if there is no distortion from O_h symmetry.

$$a_g: \psi_{320}$$

$$e_g(t_{2g}): \begin{cases} \sqrt{\frac{2}{3}}\,\psi_{322} + \sqrt{\frac{1}{3}}\,\psi_{32-1} \\ \sqrt{\frac{2}{3}}\,\psi_{32-2} - \sqrt{\frac{1}{3}}\,\psi_{321} \end{cases}$$

$$e_g(e_g): \begin{cases} \sqrt{\frac{1}{3}}\,\psi_{322} - \sqrt{\frac{2}{3}}\,\psi_{32-1} \\ \sqrt{\frac{1}{3}}\,\psi_{32-2} + \sqrt{\frac{2}{3}}\,\psi_{321} \end{cases}$$

$$f(a_g) = \langle j_0\rangle - \tfrac{5}{7}(3\cos^2\theta - 1)\langle j_2\rangle + \tfrac{9}{28}(35\cos^4\theta - 30\cos^2\theta + 3)\langle j_4\rangle,$$

$$f\{e_g(t_{2g})\} = \langle j_0\rangle + \tfrac{5}{14}(3\cos^2\theta - 1)\langle j_2\rangle - \tfrac{1}{28}(35\cos^4\theta - 30\cos^2\theta + 3)\langle j_4\rangle + \tfrac{5}{\sqrt{2}}(\sin^3\theta\cos\theta\cos 3\varphi)\langle j_4\rangle,$$

$$f\{e_g(e_g)\} = \langle j_0\rangle - \tfrac{1}{8}(35\cos^4\theta - 30\cos^2\theta + 3)\langle j_4\rangle - \tfrac{5}{\sqrt{2}}(\sin^3\theta\cos\theta\cos 3\varphi)\langle j_4\rangle.$$

Here the values of the $\langle j_n\rangle$'s are tabulated in *International Tables for X-ray Crystallography* (1974), and θ and φ are the angular coordinates of the scattering vector (Weiss & Freeman, 1959; Iwata, 1977). Even if the site symmetry is significantly distorted to D_{3d}, the distribution of d electrons is described with the above wavefunctions by changing the electron population of each level. Therefore, the structure was refined by including the populations of the d electrons at the respective levels in the parameters to be refined. The total number of $3d$ electrons of Co^{2+} was fixed at seven. The R and R_w values were reduced to 0·0124 and 0·0127, giving the populations 1·47 (8), 3·52 (8) and 2·01 (9), for a_g, $e_g(t_{2g})$ and $e_g(e_g)$ orbitals, respectively. The smallest density was obtained for the $e_g(e_g)$ orbitals, as expected.

The energy levels of the d orbitals were estimated on the assumption of the C_3 crystal field, where the point charges were placed at the octahedral O^{2-} sites, at the three nearest Co^{2+} ion sites and at the nearest Ti^{4+} ion site on the z axis. The calculation showed that the a_g orbital is the lowest, giving values of −6·34, −4·73 and 7·90 eV (1 eV = $1\cdot60\times10^{-19}$ J) for the a, $e(t_{2g})$ and $e(e_g)$ orbitals, respectively. The result of the population analysis contradicts this order of the energy levels. Therefore, structure refinement was tried by utilizing the scattering factors for the $3d$ wavefunctions based on the real crystal field C_3 described above. The wavefunctions obtained are as follows.

$$a: \psi_{320}$$

$$e(t_{2g}): \begin{cases} 0\cdot8216\psi_{322} + (0\cdot5651 + 0\cdot0749i)\psi_{32-1} \\ 0\cdot8216\psi_{32-2} - (0\cdot5651 - 0\cdot0749i)\psi_{321} \end{cases}$$

$$e(e_g): \begin{cases} 0\cdot5701\psi_{322} - (0\cdot8145 + 0\cdot1079i)\psi_{32-1} \\ 0\cdot5701\psi_{32-2} + (0\cdot8145 - 0\cdot1079i)\psi_{321} \end{cases}$$

Examination of these wavefunctions revealed that each gives an electron density distribution approximately identical to that given by the wavefunction of the corresponding orbital with O_h symmetry. In fact, refinement with the new wavefunctions gave identical populations for the respective orbitals within the experimental errors.

The final atomic parameters are listed in Table 2 together with the extinction parameters.*

Table 2. *Final parameters for* $(Co_{0\cdot95}Ti_{0\cdot05})(Ti_{0\cdot95}Co_{0\cdot05})O_3$ *after the ASF refinement*

The form of the anisotropic temperature factor is defined as $\exp\{-2\pi^2[(h^2+k^2)a^{*2}U_{11} + l^2c^{*2}U_{33} + \frac{1}{2}hka^{*2}U_{11}]\}$.

Positional and thermal parameters (Å²)

Co	z	0·355107 (9)	O	x	0·31623 (8)
	U_{11}	0·00516 (3)		y	0·02091 (8)
	U_{33}	0·00610 (5)		z	0·24588 (3)
Ti	z	0·14558 (1)		U_{11}	0·00479 (9)
	U_{11}	0·00457 (4)		U_{22}	0·00543 (9)
	U_{33}	0·00444(4)		U_{33}	0·00578 (9)
				U_{12}	0·00220 (7)
				U_{13}	0·00028 (7)
				U_{23}	0·00128 (7)

Extinction parameters (10^{-4} cm)

G_{11}	98 (20)
G_{22}	41 (2)
G_{33}	146 (11)
G_{12}	−41 (6)
G_{13}	4 (11)
G_{23}	41 (4)

Electron populations

a	1·46 (8)
$e(t_{2g})$	3·53 (8)
$e(e_g)$	2·01 (9)

Discussion

Fig. 1 shows the interatomic distances in the CoO_6 and TiO_6 octahedra. In accordance with the larger ionic radius of Co^{2+} compared with that of Ti^{4+}, the

* Lists of structure factors and Fig. 3 have been deposited with the British Library Lending Division as Supplementary Publication No. SUP 38944 (20 pp.). Copies may be obtained through The Executive Secretary, International Union of Crystallography, 5 Abbey Square, Chester CH1 2HU, England.

CoO_6 octahedron has a larger mean metal–O distance (2·113 Å) than the TiO_6 octahedron (1·979 Å). The O–O^{ii} distance on the shared face is the shortest among the O–O edges of the CoO_6 octahedron, whereas the shared edge O–O^{vi} is the shortest in the TiO_6 octahedron. Owing to the strong electrostatic repulsion, the Co^{2+} and Ti^{4+} ions are largely shifted towards the vacant octahedral sites from the centers of the respective octahedra. Especially in the TiO_6 octahedron, the ratio of the bond length between the Ti and O atoms on the shared face to that between the Ti and O atoms on the opposite face is quite large (1·115) compared to the ratios in other ilmenite-type and corundum-type crystals. For example, the values are 1·058 in the CoO_6 octahedron of the present crystal, 1·109 and 1·080 for the TiO_6 and MnO_6 octahedra in $MnTiO_3$ (Kidoh, Tanaka, Marumo & Takei, 1983), 1·020 in Ti_2O_3 (Vincent, Yvon, Grüttner & Ashkenazi, 1980), 1·041 in V_2O_3 (Vincent, Yvon & Ashkenazi, 1980) and 1·063 in Al_2O_3 (Lewis, Schwarzenbach & Flack, 1982).

Fig. 2 shows the deformation densities after the refinement with spherical scattering factors. There are six negative and eight positive peaks around the Co site. The negative peaks are on the Co–O bonds at distances of 0·48 Å from the Co site on the side of the shared face and 0·50 Å on the other side. The depths of the peaks are $-0{\cdot}49$ e Å^{-3} for the former and $-0{\cdot}78$ e Å^{3} for the latter. One of the positive peaks lies on the threefold axis at 0·61 Å from the Co site on the side of the shared face, having a height of 0·54 e Å^{-3}. On the opposite side of the Co^{2+} ion, there is a positive peak at 0·35 Å from it and with height 0·63 e Å^{-3}. The remaining six positive peaks also lie on the lines avoiding ligands at 0·42 Å (with heights of 0·91 e Å^{-3}) and 0·39 Å (heights 0·66 e Å^{-3}) from the Co site. These features resemble those observed in γ-Co_2SiO_4 (Marumo, Isobe & Akimoto, 1977), indicating the aspherical distribution of $3d$ electrons in an octahedral field. In fact, residual densities around the Co^{2+} ion largely diminished after the ASF refinement assuming the C_3 crystal field (Fig. 3).*

Around the Ti site, four large positive peaks are observed in Fig. 2. Three are at 0·52 Å from the Ti site on the Ti–O bonds pointing towards the shared face, having heights of 0·81 e Å^{-3}. The remaining one lies on the threefold axis at 0·63 Å from the Ti site, also on the side of the shared face with height 0·78 e Å^{-3}. High positive ridges connect the former three peaks to the peak on the threefold axis. A negative peak with depth $-0{\cdot}88$ e Å^{-3} exists between the Ti site and the positive peak on the threefold axis. The Ti^{4+} ion is located on the lower slope of this negative peak. In the case of Ti_2O_3, the repulsion between two Ti^{3+} ions across the shared face is relieved partly by the deformation of the coordination octahedra accompanying shifts of the central metal ions, and partly by $3d$ electrons occupying d_{z^2} orbitals which have lobes along the metal–metal line (Vincent, Yvon, Grüttner & Ashkenazi, 1980). In the present crystal, the Ti^{4+} ion has no $3d$ electrons, and the metal–metal repulsion should be cancelled mainly by deformation of the coordination octahedra. However, the positive and negative peaks near the Ti site on the threefold axis suggest that the electron cloud of the Ti^{4+} ion is deformed and spread towards the Co^{2+} ion to relieve the metal–metal repulsion. Recently a similar deformation map has been obtained for this substance by Kogure & Takeuchi (1983). The effect is small in the CoO_6 octahedron, probably owing to its larger size.

No residual densities which indicate metal–metal bonding or the covalency of the bonds between the

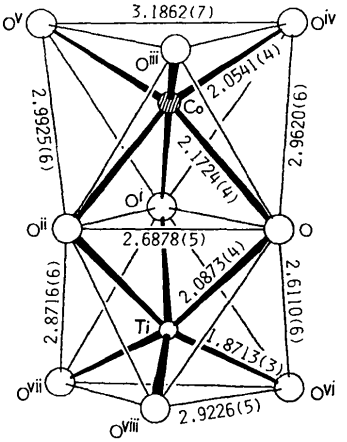

Fig. 1. Bond lengths (Å) in the CoO_6 octahedron and TiO_6 octahedron. Symmetry code: none x, y, z; (i) $-y, x-y, z$; (ii) $y-x, -x, z$; (iii) $\frac{1}{3}-x, \frac{2}{3}-y, \frac{2}{3}-z$; (iv) $\frac{1}{3}+y, \frac{2}{3}-x+y, \frac{2}{3}-z$; (v) $\frac{1}{3}+x-y, \frac{2}{3}+x, \frac{2}{3}-z$; (vi) $\frac{2}{3}-x, \frac{1}{3}-y, \frac{1}{3}-z$; (vii) $\frac{2}{3}+y, \frac{1}{3}-x+y, \frac{1}{3}-z$; (viii) $\frac{2}{3}+x-y, \frac{1}{3}+x, \frac{1}{3}-z$.

* See deposition footnote.

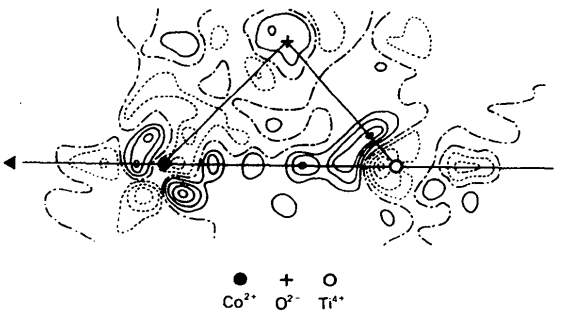

Fig. 2. The section of the difference Fourier map on the plane containing the Co^{2+}, Ti^{4+} and O^{2-} ions after the refinement with spherical scattering factors. The filled and open circles indicate the Co^{2+} and Ti^{4+} sites. The O^{2-} site is denoted with a cross. Contours are at intervals of 0·20 e Å^{-3}. Negative and zero contours are in broken and dashed–dotted lines, respectively.

metal and O atoms are observed in Fig. 2. The results of the two kinds of ASF refinements showed that the wavefunctions based on the O_h crystal field are sufficient to describe the $3d$ electron distributions in a real crystal to a first approximation.

The electron population of the a_g orbital is smaller than that of the $e_g(t_{2g})$ orbitals, contradicting the estimated energy levels. Since the energy gap between these two orbitals is small, the order of the levels may be reversed when a closer approximation is adopted in the calculation. Another possibility of obtaining the reversed electron populations exists in the processing of the diffraction data. For example, the thermal diffuse scattering and anharmonic thermal vibrations of the atoms were not taken into account in the present study.

Part of the cost was met by a Grant-in-Aid for Scientific Research, No. 56420019, from The Ministry of Education, Science and Culture, to which the authors' thanks are due.

References

BECKER, P. J. & COPPENS, P. (1974*a*). *Acta Cryst.* **A30**, 129–147.
BECKER, P. J. & COPPENS, P. (1974*b*). *Acta Cryst.* **A30**, 148–153.
BECKER, P. J. & COPPENS, P. (1975). *Acta Cryst.* **A31**, 417–425.
BOND, W. L. (1951). *Rev. Sci. Instrum.* **22**, 344.
International Tables for X-ray Crystallography (1967). Vol. II, 2nd ed. Birmingham: Kynoch Press.
International Tables for X-ray Crystallography (1974). Vol. IV. Birmingham: Kynoch Press.
IWATA, M. (1977). *Acta Cryst.* **B33**, 59–69.
KIDOH, K., TANAKA, K., MARUMO, F. & TAKEI, H. (1983). To be published.
KOGURE, H. & TAKEUCHI, Y. (1983). Private communication.
LEWIS, J., SCHWARZENBACH, D. & FLACK, H. D. (1982). *Acta Cryst.* **A38**, 733–739.
MARUMO, F., ISOBE, M. & AKIMOTO, S. (1977). *Acta Cryst.* **B33**, 713–716.
TAKEI, H., HOSOYA, S. & KOJIMA, H. (1982). *J. Jpn. Assoc. Mineral Pet. Econ. Geol.* Special Issue 3, pp. 73–82.
TOKONAMI, M. (1965). *Acta Cryst.* **19**, 486.
VINCENT, M. G., YVON, K. & ASHKENAZI, J. (1980). *Acta Cryst.* **A36**, 808–813.
VINCENT, M. G., YVON, K., GRÜTTNER, A. & ASHKENAZI, J. (1980). *Acta Cryst.* **A36**, 803–808.
WEISS, R. J. & FREEMAN, A. J. (1959). *J. Phys. Chem. Solids*, **10**, 147–161.

Acta Cryst. (1984). B**40**, 96–102

Anharmonic Thermal Vibrations of Atoms in $MgAl_2O_4$ Spinel at Temperatures up to 1933 K

BY TAKAMITSU YAMANAKA, YOSHIO TAKÉUCHI AND MASAYASU TOKONAMI

Mineralogical Institute, Faculty of Science, University of Tokyo, Hongo, Tokyo, Japan

(*Received* 25 *August* 1983; *accepted* 8 *November* 1983)

Abstract

Anharmonic thermal vibrations of atoms in $MgAl_2O_4$ spinel ($Fd3m$, $Z=4$) have been studied using sets of accurate X-ray diffraction intensities of Bragg reflections at temperatures up to 1933 K. The study was initiated by refining the temperature factor $T(\mathbf{Q})$ of each atom in the form of the second-rank tensor β_{ij}, the ellipsoidal model of harmonic vibration being assumed. Difference Fourier maps based on the structure factors obtained from the refinements at 293 K ($R=0{\cdot}0197$), 1503 K ($R=0{\cdot}0413$), 1663 K ($R=0{\cdot}0432$) and 1933 K ($R=0{\cdot}0431$) revealed residual electron densities around the atoms at the tetrahedral site A (point symmetry $\bar{4}3m$) and octahedral site B ($\bar{3}m$) and also around the O atoms ($3m$), the models of occurrence suggesting anharmonic atomic thermal vibration. The observed intensities I_{obs} ($=I_{Bragg}+I_{TDS}$) were corrected for thermal diffuse scattering to extract the real intensities of the Bragg reflections. The correction was based on the one-photon and first-order acoustic vibration model. For the anharmonic refinement, a cumulant expansion of $T(\mathbf{Q})$ in the form $T(\mathbf{Q})=\exp[\sum_n (i^n/n!)\psi_{pqrs}\ldots q_p q_q q_r q_s\ldots]$ [Johnson (1969). *Acta Cryst.* **A25**, 187–194] was adopted. The coefficients of the anharmonic tensors of both tetrahedrally and octahedrally coordinated atoms were evaluated simultaneously at each temperature: 293 K ($R=0{\cdot}014$), 1503 K ($R=0{\cdot}027$), 1663 K ($R=0{\cdot}032$) and 1933 K ($R=0{\cdot}025$). In the difference Fourier maps after the anharmonic refinements, the above-mentioned residual electron densities disappeared. As the O positional parameters ($x\,x\,x$) have been found to be unaffected by the TDS correction, the A–O and B–O interatomic distances remain unchanged. These distances are, however, changed after the refinement for the anharmonic thermal vibrations of the atoms.

Introduction

According to the Debye–Waller theory assuming harmonic thermal motion of atoms, the temperature factor W_k is given by

$$W_k=\frac{8\pi^2\sin^2\theta}{\lambda^2}\langle u_k^2\rangle=B_k\sin^2\theta/\lambda^2, \qquad (1)$$

0108-7681/84/020096-07$01.50